DETERMINATION OF CHLOROPHYLL CONTENT IN SELECTED GRASS COMMUNITIES OF KRKONOŠE MTS. TUNDRA BASED ON LABORATORY SPECTROSCOPY AND AERIAL HYPERSPECTRAL DATA

L. Červená [1*], G. Pinlová [1], Z. Lhotáková [2], E. Neuwirthová [2], L. Kupková [1], M. Potůčková [1], J. Lysák [1], P. Campbell [3,4], J. Albrechtová [2]

[1] Department of Applied Geoinformatics and Cartography, Faculty of Science, Charles University, Albertov 6, Prague 2, Czech Republic - (lucie.cervena, gabriela.pinlova, lucie.kupkova, marketa.potuckova, jakub.lysak)@natur.cuni.cz
[2] Department of Experimental Plant Biology, Faculty of Science, Charles University, Albertov 6, Prague 2, Czech Republic - (zuzana.lhotakova, eva.neuwirthova, albrecht)@natur.cuni.cz
[3] University of Maryland Baltimore County (UMBC), MD, USA,
[4] NASA Goddard Space Flight Center, MD, USA - petya@umbc.edu

Commission III, WG III/4

KEY WORDS: leaf chlorophyll content, canopy chlorophyll content, green LAI, laboratory and image spectroscopy, Krkonoše Mts., grasses, tundra

ABSTRACT:

The study focuses on the determination of chlorophyll content in four prevailing grasses in the relict arctic-alpine tundra located in the Krkonoše Mountains National Park, Czech Republic. We compared two methods for determination of leaf chlorophyll content (LCC) – spectrophotometric determination in the laboratory, and the LCC assessed by fluorescence portable chlorophyll meter CCM-300. Relationships were established between the LCCs and vegetation indices calculated from leaf spectra acquired with contact probe coupled with an ASD FieldSpec4 Wide-Res spectroradiometer. Canopy chlorophyll contents (CCC) were computed from the LCCs and green leaf area index (LAI), and modelled based on the field spectra measured by the spectroradiometer and the hyperspectral images acquired by Headwall Nano-Hyperspec® mounted on the DJI Matrice 600 Pro drone. The calculations are performed on datasets acquired in June, July and August 2020 together and separately for species and months. In general, the correlations based on June datasets work the best at both levels: median R^2 for all indices was 0.52 for all species together at leaf level and median $R^2 = 0.47$ at the canopy level (vegetation indices computed from field spectra). Canopy chlorophyll content map was created based on the results of stepwise multiple linear regression. The R^2 was 0.42 when using four wavelengths from the red and red edge spectral region. We attribute the weak model performance to a combination of several factors: leaf structure may bias LCC from laboratory measurements, effects of LAI variability on CCC, and the sampling design, probably not covering the whole phenology equally for all studied species.

1. INTRODUCTION

Chlorophyll content is considered as one of the key indicators of photosynthetic activity and thus the overall health of the plant. It changes dynamically based on the age of the leaves, illumination and also the environmental conditions. The ongoing global climate change severely alters the environmental conditions in the mountain ecosystems and especially in the ecosystems above the timberline. These ecosystems are affected primarily by increased temperatures, reduced snow cover and also by human disturbances (Klanderud, 2005; Reynolds and Tenhunen, 1996). The relict arctic-alpine tundra located in the Krkonoše Mountains National Park, the Czech Republic (50.5°N, 15.5°E, altitude above 1,350 m a. s. l.) is a unique ecosystem containing arctic as well as alpine flora and fauna and various endemic species. Three main types of tundra can be recognised there – cryo-eolian / lichen tundra on the tops of the highest mountains (mosses, lichens and alpine heathlands), vegetated-cryogenic / grassy tundra on the plateaus near the Luční bouda and the Labská bouda chalets (Pinus mugo scrub, peat bogs and closed alpine grasslands dominated with Nardus stricta and subalpine tall grasslands) and niveo-glacigenic / flower-rich tundra in the glacier corries (Kociánová et al., 2015; Soukupová et al., 1995). The grassy tundra covers a substantial part of the area and changes in its vegetation composition have already been documented – besides expansion of Pinus mugo (Štursa and Wild, 2014) and Norway spruce (Treml et al., 2012) the spread of competitive grasses Calamagrostis villosa (Hejcman et al., 2009) and Molinia caerulea (Hejcman et al., 2010) at the expense of the closed alpine grassland dominated with Nardus stricta was observed. The seasonal and annual trends in chlorophyll contents in these grass species could help to better understand ongoing ecosystem changes.

The leaf chlorophyll content (LCC) can be determined by laboratory methods consisting of pigment extraction into an organic solvent followed by spectrophotometric evaluation (e. g. Porra et al., 1989; Wellburn, 1994). This method is considered to be precise and reliable but it is destructive and time-demanding. The non-destructive methods are based on the specific optical properties of the chlorophyll. The spectroscopic approaches use the leaf clip in the field or the contact probe or integrating sphere in the laboratory. Computation of vegetation indices referring to the leaf chlorophyll content follows. The

---

* Corresponding author

devices called portable chlorophyll meters represent another possibility. They directly quantify the transmittance or fluorescence on the wavelengths affected by the pigment content. The advantage of fluorescence-based chlorophyll meters (e.g. CCM-300) is the ability to measure narrow or small leaves without the requirement to cover the entire measurement area.

Remote sensing offers methods suitable to monitor chlorophyll content in larger areas. Based on the methods of image and field spectroscopy we estimate canopy chlorophyll content (CCC), defined as the product of LCC and leaf area index (LAI) or green LAI (which takes into account only the green parts of the plants). However, to be able to obtain the CCC from the images using empirical regressions or radiative transfer modelling, we still need reliable training data of LCC and (green) LAI collected in the field. Standard procedures are well established for vegetation traits assessment for forests (Croft et al., 2014) and agriculture crops (Croft et al., 2020). However, natural heterogeneous grasslands are studied less frequently (e. g. Darvishzadeh et al., 2008a)

The main aim of this paper is to estimate CCC for four dominant grass species of grassy arctic-alpine tundra in Krkonoše Mts. (*Nardus stricta*, *Molinia caerulea*, *Calamagrostis villosa* and *Deschampsia cespitosa*) using the hyperspectral images acquired by Headwall Nano-Hyperspec® mounted on the DJI Matrice 600 Pro drone and empirical modelling. The addressed research questions are:

1) Can we obtain comparable results for LCC measured destructively in the laboratory and non-destructively by the CCM-300 chlorophyll meter in the field? What will be the performance of the empirical models for leaf spectra acquired by the contact probe coupled with the spectroradiometer ASD FieldSpec4 Wide-Res?

2) Are the vegetation indices calculated from the field spectra (spectroradiometer ASD FieldSpec4 Wide-Res) and from the image spectra (Headwall Nano-Hyperspec®) comparable? What are the most suitable indices for estimation of CCC?

2. DATA AND METHODS

2.1 Data

The vegetation season in Krkonoše Mts. tundra is very short. It lasts from June to September, and so the field campaigns were held in the middle of June, July and August 2020. Six permanent plots with a diameter of approx. 2 m for each of four species (*Nardus stricta*, *Molinia caerulea*, *Calamagrostis villosa* and *Deschampsia cespitosa*) have been defined (Figure 1). In every field campaign within each permanent plot two subplots with dimensions of 10 cm x 10 cm were randomly selected (i.e. 48 subplots in every term: 4 species x 6 plots x 2 subplots). The position of the centre of each sup-plot was surveyed with the geodetic GNSS receiver. Three field spectra of subplot and its closest surrounding were acquired using the spectroradiometer ASD FieldSpec4 Wide-Res from approximately 0.5 m height above the canopy (i.e. a circle with a diameter of 22 cm on the ground) and a median spectrum was calculated. Two leaves from the subplot were measured in one third of the leaf length from the apex by the CCM-300 (OptiSciences, Inc., Hudson, NH, USA). Leaf chlorophyll was extracted from samples of the

same two leaves in the laboratory spectrophotometrically according to Porra et al. (1989) and Wellburn (1994). In the following text, we refer with "lab" the biochemically assessed chlorophyll content in laboratory and with "CCM-300" the chlorophyll content assessed by fluorescence portable chlorophyll meter CCM-300. All the biomass from the subplot was collected, put in the zip lock bags and placed into the cooling box on ice for transport to the lab. In the laboratory it was sorted separating green mass and necromass. All the green leaves were weighed. Several green leaves were scanned and weighed to get the ratio of leaf area and weight which was then used to compute the green LAI based on the weight of all the green leaves from the subplot 10 cm x 10 cm. Several green leaves were also measured by the contact probe (spot size 10 mm) coupled with spectroradiometer ASD FieldSpec4 Wide-Res (Figure 2) to obtain leaf reflectance spectra – every sample was measured in five positions and then the median spectrum was calculated. The reflectance spectra (field and laboratory) acquired by the ASD FieldSpec4 Wide-Res spectroradiometer have 2,151 bands within the spectral range 350 – 2,500 nm.
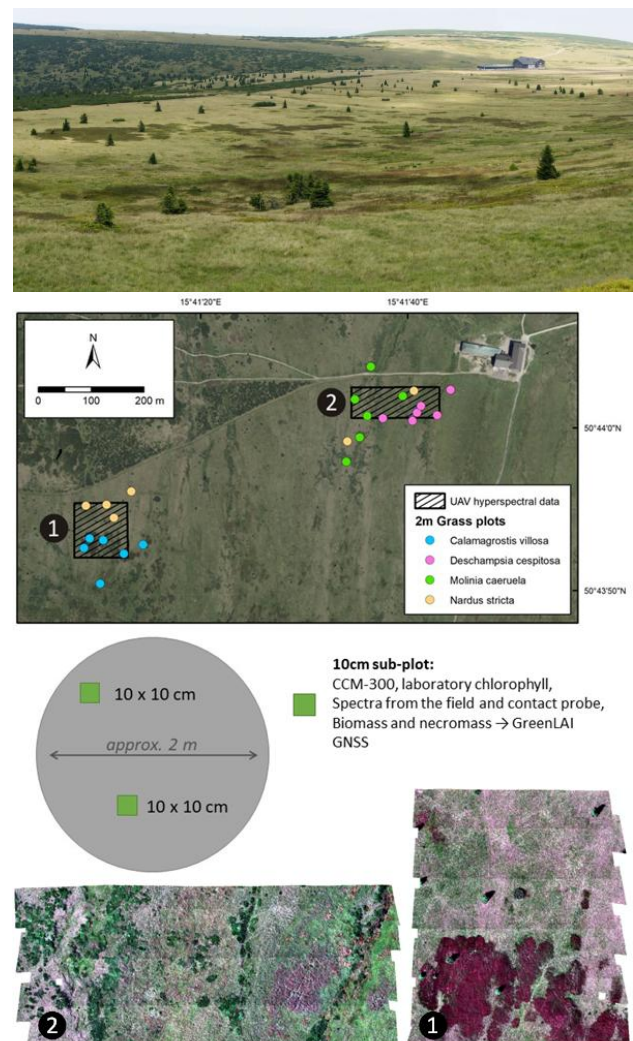

Figure 1. The study area of the grassy tundra around the Luční bouda chalet (up), the sampling design (in the middle) and the examples of Headwall Nano-Hyperspec® data acquired in August 2020 for both test areas (bottom)

Figure 2. Leaf spectra measurements – the examples of samples of *Calamagrostis villosa* (upper left), *Molinia caerulea* (upper right), *Deschampsia cespitosa* (bottom left) and *Nardus stricta* (bottom right)

At each field campaign hyperspectral images were acquired using Headwall Nano-Hyperspec® mounted on the DJI Matrice 600 Pro drone. Radiometric and basic geometric corrections were performed in the Headwall SpectralView – Hyperspec v3.1.0 software. Precise georeferencing and mosaicking were performed by manual addition of tie points in the ArcGIS for desktop software. The radiometric corrections were performed using the portable 3 m x 3 m fabric target placed in the scanned area (Group 8 Technology, Inc., Provo, UT, USA), however, the target is included only in one flight line and the calibration is used for the whole area. The data cube consists of 269 bands, with wavelength ranging from 400 to 1,000 nm. Spatial resolution is 3 cm, which was resampled to 9 cm to have similar dimension as the subplots. More details about the procedures of Headwall Nano-Hyperspec® data pre-processing can be found in Červená et al. (2020a)

2.2 Methods

To answer the first objective, the correlation of LCC measured destructively in the laboratory (further abbreviated as LCC_lab) and non-destructively by the CCM-300 chlorophyll meter in the field (further abbreviated as LCC_CCM-300) was performed for all the species together and for each species separately. Our preliminary results indicate that significant differences in both methods of LCC measurements were observed (Figure 3, Table 2). Thus, all the subsequent correlations with the chlorophyll indices calculated from the leaf spectra acquired by the contact probe were performed for both methods of chlorophyll measurements. The vegetation indices were selected based on the Main et al. (2011) and le Maire et al. (2004) – the original references can be found in Table 1.

Several steps had to be taken to fulfil the second objective. For the comparison of the spectra acquired on the canopy level, i.e. measured by the spectroradiometer in the field and the image spectra acquired by the hyperspectral camera on the drone, the field data were spectrally resampled using spectral response with gaussian density function to the same spectral resolution of 11.2 nm (it corresponds to five adjacent bands in the Nano-Hyperspec® data). Our experimental results showed that this reduction of spectral bands decreases the noise and the correlations of bands in the hyperspectral image data and improves the results (Červená et al., 2020b). Based on these

resampled data, the selected chlorophyll indices (same set which was used for the leaf level spectra, Table 1) were calculated and compared using the correlations and coefficients of determination.

Index	Level	Reference
Carter4	L	Carter (1994)
Datt	L	Datt (1999)
Datt2	L	Datt (1999)
DD	L	le Maire et al. (2004)
Gitelson	L	Gitelson et al. (1999)
Gitelson2	L	Gitelson et al. (2003)
Maccioni	L	Maccioni et al. (2001)
MCARI2	C	Wu et al. (2008)
MCARI2/OSAVI2	C	Wu et al. (2008)
MCARI/OSAVI	C	Daughtry (2000)
MTCI	C	Dash and Curran (2004)
NDVI	C	Tucker (1979)
NDVI2	L	Gitelson and Merzlyak (1997)
OSAVI	C	Rondeaux et al. (1996)
OSAVI2	C	Wu et al. (2008)
PSND	L	Blackburn (1998)
PSSR	L	Blackburn (1998)
REP_LI	L	Guyot and Baret (1988)
SR6	L	Zarco-Tejada and Miller (1999)
TCARI	C	Haboudane et al. (2002)
TCARI/OSAVI	C	Haboudane et al. (2002)
Vogelmann	L	Vogelmann et al. (1993)
Vogelmann2	L	Vogelmann et al. (1993)

Table 1. The selected chlorophyll indices with the level from which they were retrieved (L = leaf, C = canopy) and the reference. Adapted after Main et al. (2011) and le Maire et al. (2004).

The next step was a computation of the canopy chlorophyll content (CCC), which is calculated by multiplying green LAI and LCC. In our case we have two different measurements of LCC, so we have also two sets of CCCs further abbreviated as CCC_lab (the laboratory determination of LCC) and CCC_CCM-300 (the CCM-300 readings of LCC) using the default built-in calibration.

Empirical models between both CCCs and vegetation indices computed from the field spectra were calculated using simple linear regressions for the available combinations of species and terms. Empirical models using the spectra from the hyperspectral camera were calculated only for all the terms together because the image data does not cover all the plots, so the number of samples per month would be too small.

Since the empirical models based on vegetation indices did not give convincing results, a stepwise multiple linear regression was also computed for the image spectra and CCC_lab. Multiple stepwise regression is a method which tries to find the optimal model by adding or subtracting the independent variables step by step. The objective is to maximise the prediction power with the least number of independent variables (wavelengths) which are statistically relevant for the prediction of the dependent variable values (CCC). For our model 4 wavelengths were used. The 10 fold cross-validation was also computed.

The main goal was to create chlorophyll maps for selected grass species. The hyperspectral image data were firstly classified to produce a mask of the studied grass species. The maximum likelihood classifications were used. They were run using the training data collected in the field by the botanists and 10 bands

resulting from minimum noise fraction transformation of all three hyperspectral images per every site. The overall accuracies assessed by the validation points reached about 90 % for both classifications (Ježek, 202x). The classifications results were filtered by the 3x3 kernel to eliminate the isolated pixels and then the masks were created. The equation from the multiple stepwise regression was applied to the masked hyperspectral image data from all the terms.

All the main computations were performed using the R software and the hsdar package (Lehnert et al., 2019). Also ENVI 5.5, ArcGIS for desktop and Microsoft Excel were used for data preparation and visualisation.

3. RESULTS AND DISCUSSION

3.1 LCC

Significant differences in both destructive and non-destructive methods of LCC measurements were observed (Figure 3, Table 2). We can see in the Figure 3 that values of LCC_lab are generally higher than the values of LCC_CCM-300. The correlations between both LCCs were evaluated by the coefficients of determination, which across all species and terms reached the value of 0.46 (Table 2). Since the chlorophyll content is species dependent, it is necessary to evaluate the relationships between LCCs also for the individual species. The best results were observed for *Calamagrostis villosa* ($R^2 = 0.66$ for the entire study period, however on a relatively small range of LCC, approximately 200 mg/m^2). *Molinia caerulea* shows an increase in LCC_lab during the season, but the same trend cannot be seen in the LCC_CCM-300. Very good correlation between the two methods of measuring LCC in *Molinia caerulea* can be observed only in June ($R^2 = 0.70$). These results can be compared with the results of the undergraduate thesis of Pinlová (2019), where the leaves of *Molinia caerulea* grown in pots were measured with the CCM-300 and the laboratory method at an early stage of growth, and the results showed a significant linear relationship with a coefficient of determination of 0.94. *Deschampsia cespitosa* reached the highest LCC values in case of both methods of measurements, nevertheless, their correlation is very low ($R^2 = 0.04$ for the entire season, the result for the separate months are slightly better). *Nardus stricta* is the most difficult grass to measure (due to its narrow rolled leaves) and its LCCs are highly variable. The different results for all the grasses can potentially be explained by different anatomical structures of their leaves (see the Figure 4), which can complicate the recalculation of chlorophyll per leaf area. Flat leaves of *Calamagrostis villosa, Deschampsia cespitosa,* and *Molinia caerulea* are easy to scan and get almost unbiased leaf area. In contrast, *Nardus stricta* rolled leaves are hard to expand and the leaf area acquired by scanning may be underestimated, which brings bias into the area-based LCC. We addressed this issue by introducing a correction factor from microscopic images of *Nardus stricta* leaves, which was used for correction of scanned projection leaf area to real leaf area. The grass leaf structure could also bias the CCM-300 readings as the default calibration relationship between measured fluorescence ratio and chlorophyll content reading was trained on broadleaved woody species (Gitelson et al., 1999). Some bias in chlorophyll meter readings could be also seen in CCM-300 data distribution, which deviates from the normal towards the bimodal (Figure 3).

The results from the August measurements (data not shown) suggest that the LCC at all subplots for one species are very similar and the LCC values are more affected by differences among leaves and measurements, than by the location. Based on this finding, it can be assumed that it will be possible to estimate the grass species based on leaf chlorophyll content, however, the quantitative estimation of LCC in the given grass species will be very problematic due to the high variability of the data over a small range of LCC values.

	All months	**June**	**July**	**August**
All species	0.46	0.51	0.34	0.65
C. V.	0.66	0.52	0.83	0.93
D. C.	0.04	0.18	0.21	0.33
M. C.	0.19	0.70	0.02	0.22
N. S.	0.03	0.15	0.17	0.00

Table 2. The coefficients of determination (R^2) produced by the correlations of LCC measured destructively in the laboratory and non-destructively by the CCM-300 chlorophyll meter in the field (*C.V. – Calamagrostis villosa, D.C. – Deschampsia cespitosa, M.C. – Molinia caerulea, N.S. – Nardus stricta*)
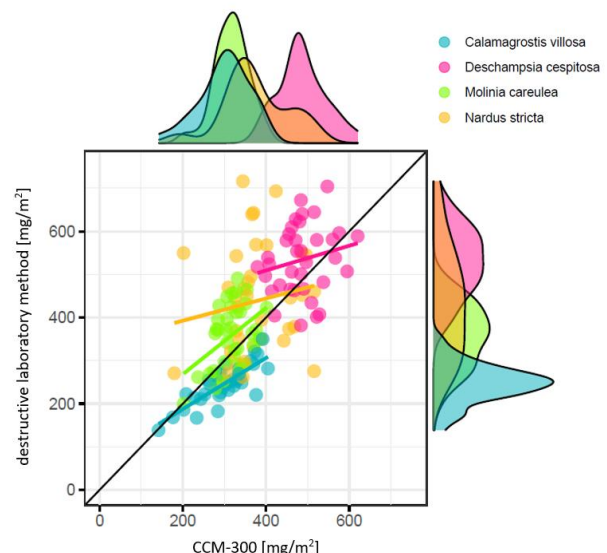

Figure 3. Leaf chlorophyll content values measured with CCM-300 chlorophyll meter in the field and determined biochemically in the laboratory

Next step on the leaf level was to evaluate the correlations of the LCC (both destructive and non-destructive determinations) with the selected chlorophyll indices (Table 1) calculated from the reflectance spectra measured by the spectroradiometer coupled with the contact probe in the laboratory. Very weak correlations were gained basically for all combinations of input data. Statistically significant results were achieved only for LCC_lab and the most chlorophyll indices for all the species together in June (the median of R^2 is 0.52, the best $R^2 = 0.66$ was reached by Gitelson index). However, the individual species show essentially no correlations in June. These findings may be related to the different phenology and rates of development of individual species at the beginning of the vegetation season. This

hypothesis can be also supported by the similar trend for data from July – the median of R^2 was 0.46 for all species together but there were no correlations within a species. As for the individual species, the best correlation results show *Calamagrostis villosa* for both methods of LCC measurement in August (i.e., LCC_lab: the median $R^2 = 0.41$, the best $R^2 = 0.54$ for NDVI2 and OSAVI2; LCC_CCM-300: the median $R^2 = 0.36$, the best $R^2 = 0.53$ for NDVI and OSAVI). This result can be explained by the fact that our sampling terms covered the full phenology of this species including the beginning of the senescence. The senescence phase in *Calamagrostis villosa* is very visible on this species and often varies among the different grass clusters – the top parts of the leaves can be drier, become violet or at least have the violet dots on the leaves, partly due to accumulation of purple protective pigments anthocyanins and spot necroses. Surprisingly, good results of correlations were also reached for *Nardus stricta* and LCC_lab for June (median $R^2 = 0.38$, the best $R^2 = 0.53$ for PSND) and August (median $R^2 = 0.49$, the best $R^2 = 0.59$ for REP_Li). All these results are, thus, affected by quite a small number of samples – only 12 when looking at one species in one term, but a more extensive sampling would be very time and labour consuming. We expected that the best results of the correlations will be for individual species during the whole season, but this was not confirmed.
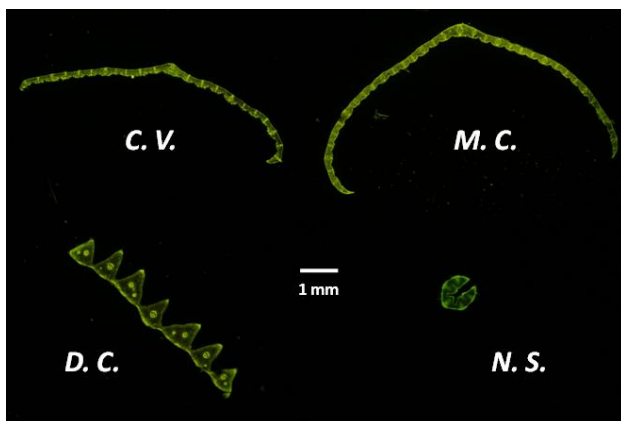

Figure 4. Anatomical sections of all the studies species – examples from August 2020. Hand-microtome fresh leaves sections treated with Naturstoff reagent A and acquired under blue light excitation. Yellow – fenolic compounds fluorescence. (*C.V. – Calamagrostis villosa, D.C. – Deschampsia cespitosa, M.C. – Molinia caerulea, N.S. – Nardus stricta*). Photo author Lena Hunt (Charles University).

3.2 CCC

The selected indices often used for the chlorophyll content estimations (Table 1) were calculated based on the spectral data (field spectroradiometer and hyperspectral camera) resampled to 54 bands in the spectral range 400 – 1,000 nm. Afterwards, indices calculated from the field spectra and indices calculated from the hyperspectral image data were compared using the correlations and coefficients of determination. The best results of R^2 were around 0.8 (e.g. Carter4, Vogelmann2, NDVI, MTCI) while the median R^2 was 0.75. These results indicate that the selected indices derived from the field spectra and from the image data are comparable.

The empirical models built between vegetation indices calculated from field spectra and hyperspectral image data, respectively, and both CCCs across all the terms show similar trends. The best correlations were reached for *Molinia caerulea* with median R^2 values 0.51 (CCC_lab) and 0.49 (CCC_CCM-300) for image spectra and 0.48 (CCC_lab) and 0.44 (CCC_CCM-300) for field spectra. The second best results were reached for all the species together (median R^2 values were the same for both CCCs – 0.27 for field spectra, 0.24 for image spectra). Correlation results for other species were poor. These results confirm that the relation of field and image spectra to CCC is more LAI driven than LCC driven. The same trend of LAI prevailing over LCC can be seen also in the results of correlations of vegetation indices calculated from field spectra and both CCCs for the separate months. Regardless of the LCC measurement method, we can see that the best correlations were reached for June – the correlations work quite well for all the species together (median $R^2 = 0.47$) as well as for the separate species (median R^2 of *Molinia caerulea* = 0.49, of *Calamagrostis villosa* = 0.48 and of *Deschampsia cespitosa* = 0.30) with the exception of *Nardus stricta* (median $R^2 = 0.14$). The correlations based on July and August data do not show good results. Considering the important impact of LAI for deriving CCC values, the lowest LAI values and ranges from June measurements (Figure 5) support the best model performance between CCC and field and image spectra from this part of the season. The seasonal LAI course for individual species shows that the phenology and leaf development is not synchronised among species. *Molinia caerulea* and *Nardus stricta* appear to start their growth activity later than the other two species. The LAI course also suggests that we better covered the seasonal phenology of *Calamagrostis villosa* and *Nardus stricta* than in the case of *Deschampsia cespitosa* and *Molinia caerulea* with longer vegetation seasons.
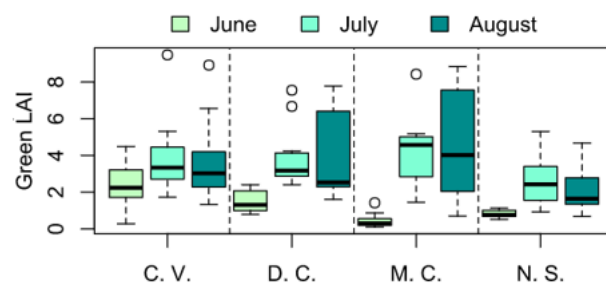

Figure 5. The green LAI during the season for individual species

The stepwise multiple linear regression computed for the image spectra and CCC_lab achieved the coefficient of determination's value 0.42 using four wavelengths (see the equation 1). The RMSE reached by 10 fold cross-validation was 833.5 mg/m^2.

$$CCC\_lab = 1904.8 + 2264.6 * R_{606} - 2130.9 * R_{617} - 366 * R_{740} + 242.9 * R_{807} \qquad (1)$$

where R_λ = reflectance at the corresponding wavelength λ

This equation was then applied to the masked hyperspectral image data from all the terms. The resulting maps of CCC can be seen in Figure 6 together with the classifications of the studied species. It is clearly visible that the CCC is very species dependent but the intraspecific variation in CCC is rather small. *Deschampsia cespitosa* has the highest LCC values of all species, which is confirmed on the chlorophyll map (Figure 6,

area 2) especially in June when the differences among the species are the biggest. The areas with low CCC values in *Deschampsia cespitosa* are caused by flowering, which is clearly visible in the hyperspectral images in some places with this species in July and August (see the Figure 1) and affects the results. Despite our best efforts to capture ideal data, weather in the mountains sometimes causes unevenness in the irradiation that can be visible in the image data. The results for area 2 from June and also July are unfortunately influenced by the uneven light condition during the scanning. The smallest values of LCC in *Calamagrostis villosa* in July are also probably caused by the light conditions inconsistency of the July data for area 1.
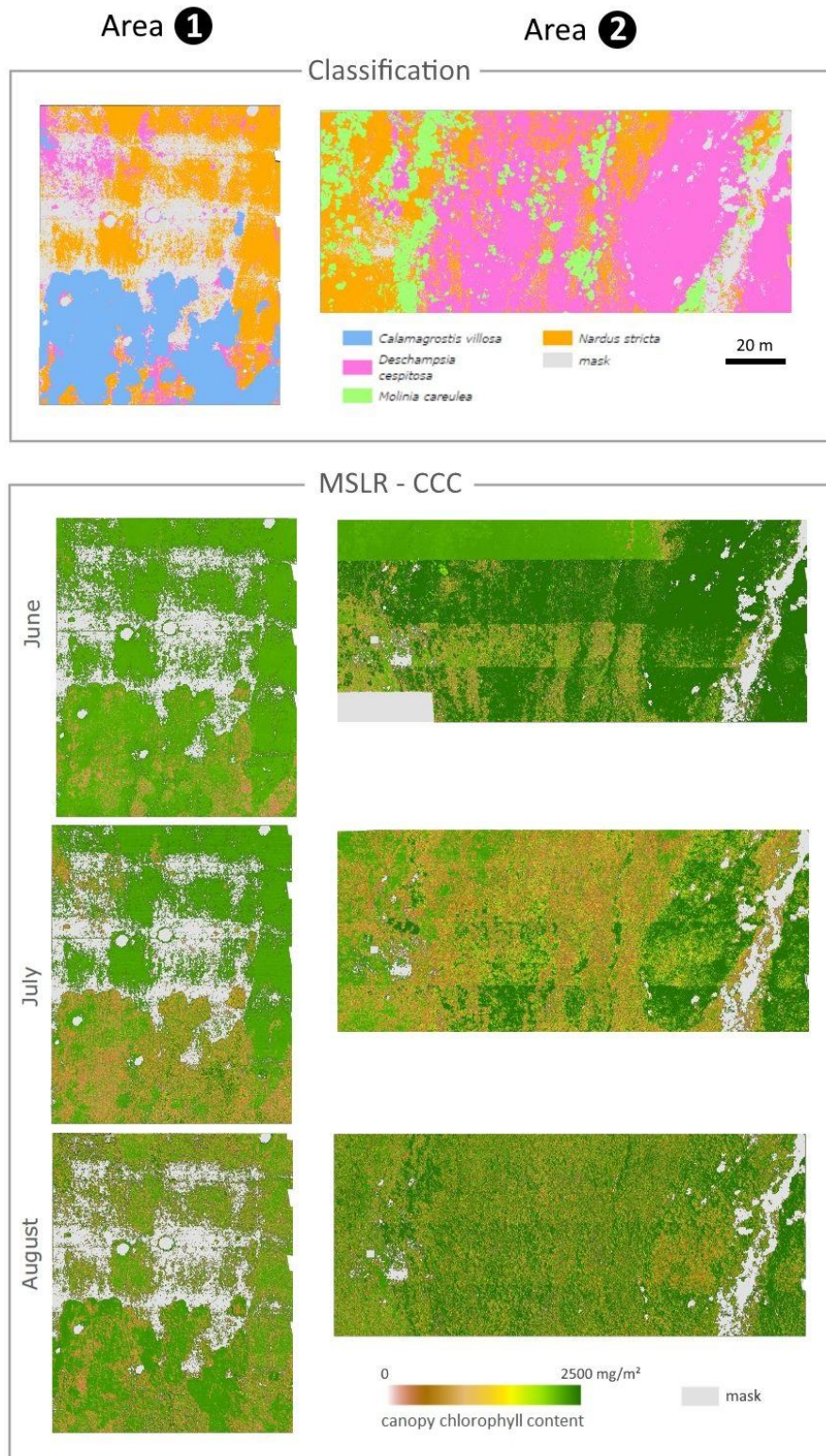

Figure 6. The species classification and the canopy chlorophyll content (CCC) map based on the stepwise multiple linear regression (MSLR - Equation 1) computed for the image spectra.

4. CONCLUSIONS

The main aim of this paper was to estimate the canopy chlorophyll content for four dominant grass species of grassy arctic-alpine tundra in Krkonoše Mts. (*Nardus stricta*, *Molinia caerulea*, *Calamagrostis villosa* and *Deschampsia cespitosa*) using the hyperspectral images acquired by Headwall Nano-Hyperspec® mounted on the DJI Matrice 600 Pro drone and empirical modelling. This objective was reached by the method of stepwise multiple linear regression computed for the image spectra and canopy chlorophyll content which was the combination of leaf chlorophyll content determined by the laboratory method and green leaf area index. The R^2 was 0.42 and the RMSE = 833.5 mg/m^2 when using four wavelengths (606, 617, 740 and 817 nm).

There were also two partial objectives. The first one was to compare the leaf chlorophyll contents derived destructively in the laboratory and non-destructively by the CCM-300 chlorophyll meter in the field and also their performances in the models with vegetation indices computed from the leaf level spectra acquired by the contact probe. The results show that leaf chlorophyll content determined by the CCM-300 is underestimated compared to laboratory values and that between both methods the significant relations do not exist for studied grasses. We hypothesise that the different leaf structure may bias the leaf area assessment and also influence the CCM-300 readings as the built-in calibration equation was trained on deciduous woody species. Unfortunately, we could not use well established transmittance-based chlorophyll meters such as SPAD frequently used in other grassland studies (e.g. Darvishzadeh et al., 2008a, 2008b), as the narrow *Nardus stricta* leaves do not cover the device´s field of view. The correlations of leaf chlorophyll contents with vegetation indices computed from the spectra measured by the contact probe coupled with the spectroradiometer achieved generally weak correlations for all combinations of input data. The only better results were achieved for destructively measured LCC and the most chlorophyll indices for all the species together in June (the median of R^2 is 0.52). The second partial objective was to compare the models calculated based on the canopy chlorophyll contents and vegetation indices derived from the field spectra and image spectra. At the canopy level the differences in the method of LCC determination were negligible, because LAI value is of higher importance than the value of LCC. The selected vegetation indices derived from the field spectra and from the image data were comparable (the best results of R^2 were around 0.8 for Carter4, Vogelmann2, NDVI and MTCI). Concerning the correlations of vegetation indices calculated from field spectra with CCC, the same finding was confirmed as for the leaf level, June dataset gave the best results. But overall the correlations were weak. In comparison to other studies focused on grassland CCC estimation from field spectra (e.g. (Zheng et al., 2021) the number of sampled subplots for field spectra measurement and covering the UAV overflight area was rather low, which may result in worse models´ performance at canopy level.

ACKNOWLEDGEMENTS

REFERENCES

Blackburn, G.A., 1998. Quantifying Chlorophylls and Caroteniods at Leaf and Canopy Scales. *Remote Sens. Environ.* 66, 273–285. doi.org/10.1016/S0034-4257(98)00059-5

Carter, G.A., 1994. Ratios of leaf reflectances in narrow wavebands as indicators of plant stress. *Int. J. Remote Sens.* 15, 697–703. doi.org/10.1080/01431169408954109

Červená, L., Kupková, L., Potůčková, M., Lysák, J., 2020a. Seasonal Spectral Separability of Selected Grasses: Case Study From The Krkonoše Mts. Tundra Ecosystem. *Int. Arch. Photogramm. Remote Sens. Spat. Inf. Sci.* XLIII-B3-2020, 371–376. doi.org/10.5194/isprs-archives-XLIII-B3-2020-371-2020

Červená, Lucie, Lysák, J., Potůčková, M., Kupková, L., 2020b. Zkušenosti se zpracováním hyperspektrálních dat pořízených UAV. *Presented at the GIS Ostrava 2020 - Prostorová data pro Smart City a Smart Region.* doi.org/10.31490/9788024843988-4

Croft, H., Arabian, J., Chen, J.M., Shang, J., Liu, J., 2020. Mapping within-field leaf chlorophyll content in agricultural crops for nitrogen management using Landsat-8 imagery. *Precis. Agric.* 21, 856–880. doi.org/10.1007/s11119-019-09698-y

Croft, H., Chen, J.M., Zhang, Y., 2014. Temporal disparity in leaf chlorophyll content and leaf area index across a growing season in a temperate deciduous forest. *Int. J. Appl. Earth Obs. Geoinformation* 33, 312–320. doi.org/10.1016/j.jag.2014.06.005

Darvishzadeh, R., Skidmore, A., Schlerf, M., Atzberger, C., 2008a. Inversion of a radiative transfer model for estimating vegetation LAI and chlorophyll in a heterogeneous grassland. *Remote Sens. Environ.* 112, 2592–2604. doi.org/10.1016/j.rse.2007.12.003

Darvishzadeh, R., Skidmore, A., Schlerf, M., Atzberger, C., Corsi, F., Cho, M., 2008b. LAI and chlorophyll estimation for a heterogeneous grassland using hyperspectral measurements. *ISPRS J. Photogramm. Remote Sens.* 63, 409–426. doi.org/10.1016/j.isprsjprs.2008.01.001

Dash, J., Curran, P.J., 2004. The MERIS terrestrial chlorophyll index. *Int. J. Remote Sens.* 25, 5403–5413. doi.org/10.1080/0143116042000274015

Datt, B., 1999. Visible/near infrared reflectance and chlorophyll content in Eucalyptus leaves. *Int. J. Remote Sens.* 20, 2741–2759. doi.org/10.1080/014311699211778

Daughtry, C., 2000. Estimating Corn Leaf Chlorophyll Concentration from Leaf and Canopy Reflectance. *Remote Sens. Environ.* 74, 229–239. doi.org/10.1016/S0034-4257(00)00113-9

Gitelson, A.A., Buschmann, C., Lichtenthaler, H.K., 1999. The Chlorophyll Fluorescence Ratio F735/F700 as an Accurate Measure of the Chlorophyll Content in Plants. *Remote Sens. Environ.* 69, 296–302. doi.org/10.1016/S0034-4257(99)00023-1

Gitelson, A.A., Gritz †, Y., Merzlyak, M.N., 2003. Relationships between leaf chlorophyll content and spectral reflectance and algorithms for non-destructive chlorophyll assessment in higher plant leaves. *J. Plant Physiol.* 160, 271–282. doi.org/10.1078/0176-1617-00887

Gitelson, A.A., Merzlyak, M.N., 1997. Remote estimation of chlorophyll content in higher plant leaves. *Int. J. Remote Sens.* 18, 2691–2697. doi.org/10.1080/014311697217558

Guyot, G., Baret, F., 1988. Utilisation de la Haute Resolution Spectrale pour Suivre L'etat des Couverts Vegetaux 287, 279.

Haboudane, D., Miller, J.R., Tremblay, N., Zarco-Tejada, P.J., Dextraze, L., 2002. Integrated narrow-band vegetation indices for prediction of crop chlorophyll content for application to precision agriculture. *Remote Sens. Environ.* 81, 416–426. doi.org/10.1016/S0034-4257(02)00018-4

Hejcman, M., Češková, M., Pavlů, V., 2010. Control of Molinia caerulea by cutting management on sub-alpine grassland. *Flora - Morphol. Distrib. Funct. Ecol. Plants* 205, 577–582. doi.org/10.1016/j.flora.2010.04.019

Hejcman, M., Klaudisová, M., Hejcmanová, P., Pavlů, V., Jones, M., 2009. Expansion of Calamagrostis villosa in sub-alpine Nardus stricta grassland: Cessation of cutting management or high nitrogen deposition? *Agric. Ecosyst. Environ.* 129, 91–96. doi.org/10.1016/j.agee.2008.07.007

Ježek, V., 202x. Remote sensing for the analysis of changes in the distribution of conservatively important grass species in tundra of the Krkonoše Mts. (Bachelor thesis in prep.). Charles University, Prague.

Klanderud, K., 2005. Climate change effects on species interactions in an alpine plant community. *J. Ecol.* 93, 127–137. doi.org/10.1111/j.1365-2745.2004.00944.x

Kociánová, M., Štursa, J., Vaněk, J., 2015. *Krkonošská tundra*. Správa Krkonošského národního parku, Vrchlabí.

le Maire, G., François, C., Dufrêne, E., 2004. Towards universal broad leaf chlorophyll indices using PROSPECT simulated database and hyperspectral reflectance measurements. *Remote Sens. Environ.* 89, 1–28. doi.org/10.1016/j.rse.2003.09.004

Lehnert, L.W., Meyer, H., Obermeier, W.A., Silva, B., Regeling, B., Bendix, J., 2019. Hyperspectral Data Analysis in R : The hsdar Package. *J. Stat. Softw.* 89. doi.org/10.18637/jss.v089.i12

Maccioni, A., Agati, G., Mazzinghi, P., 2001. New vegetation indices for remote measurement of chlorophylls based on leaf directional reflectance spectra. *J. Photochem. Photobiol.* B 61, 52–61. doi.org/10.1016/S1011-1344(01)00145-2

Main, R., Cho, M.A., Mathieu, R., O'Kennedy, M.M., Ramoelo, A., Koch, S., 2011. An investigation into robust spectral indices for leaf chlorophyll estimation. *ISPRS J. Photogramm. Remote Sens.* 66, 751–761. doi.org/10.1016/j.isprsjprs.2011.08.001

Pinlová, G., 2019. Určování obsahu chlorofylu ve vybraných travinách krkonošské tundry (Bachelor thesis). Charles University, Prague.

Porra, R.J., Thompson, W.A., Kriedemann, P.E., 1989. Determination of accurate extinction coefficients and simultaneous equations for assaying chlorophylls a and b extracted with four different solvents: verification of the concentration of chlorophyll standards by atomic absorption spectroscopy. *Biochim. Biophys. Acta BBA - Bioenerg.* 975, 384–394. doi.org/10.1016/S0005-2728(89)80347-0

Reynolds, J.F., Tenhunen, J.D., 1996. *Landscape function and disturbance in Arctic tundra*. Springer, Berlin; New York.

Rondeaux, G., Steven, M., Baret, F., 1996. Optimization of soil-adjusted vegetation indices. *Remote Sens. Environ.* 55, 95–107. doi.org/10.1016/0034-4257(95)00186-7

Soukupová, L., Kociánová, M., Jeník, J., Sekyra, J., 1995. Arctic alpine tundra in the Krkonoše, the Sudetes. *Opera Corcon.* 32, 5–88.

Štursa, J., Wild, J., 2014. Kleč a smilka – klíčoví hráči vývoje alpínského bezlesí Krkonoš (Vysoké Sudety, Česká republika). *Opera Corcon.* 51, 5–36.

Treml, V., Ponocná, T., Büntgen, U., 2012. Growth trends and temperature responses of treeline Norway spruce in the Czech-Polish Sudetes Mountains. *Clim. Res.* 55, 91–103. doi.org/10.3354/cr01122

Tucker, C.J., 1979. Red and photographic infrared linear combinations for monitoring vegetation. *Remote Sens. Environ.* 8, 127–150. doi.org/10.1016/0034-4257(79)90013-0

Vogelmann, J.E., Rock, B.N., Moss, D.M., 1993. Red edge spectral measurements from sugar maple leaves. *Int. J. Remote Sens.* 14, 1563–1575. doi.org/10.1080/01431169308953986

Wellburn, A.R., 1994. The Spectral Determination of Chlorophylls a and b, as well as Total Carotenoids, Using Various Solvents with Spectrophotometers of Different Resolution. *J. Plant Physiol.* 144, 307–313. doi.org/10.1016/S0176-1617(11)81192-2

Wu, C., Niu, Z., Tang, Q., Huang, W., 2008. Estimating chlorophyll content from hyperspectral vegetation indices: Modeling and validation. *Agric. For. Meteorol.* 148, 1230–1241. doi.org/10.1016/j.agrformet.2008.03.005

Zarco-Tejada, P.J., Miller, J.R., 1999. Land cover mapping at BOREAS using red edge spectral parameters from CASI imagery. *J. Geophys. Res. Atmospheres* 104, 27921–27933. doi.org/10.1029/1999JD900161

Zheng, F., Xu, B., Xiao, P., Zhang, X., Manlike, A., Jin, Y.-X., Li, C., Feng, X., An, S., 2021. Estimation of chlorophyll content in mountain steppe using in situ hyperspectral measurements. *Spectrosc. Lett.* 54, 495–506. doi.org/10.1080/00387010.2019.1711131